Available online at www.sciencedirect.com
SCIENCE DIRECT
Trans. Nonferrous Met. Soc. China 16(2006) 452−458
Transactions of Nonferrous Metals Society of China
www.csu.edu.cn/ysxb/

Solidification microstructural constituent and its crystallographic morphology of permanent-mould-cast Mg-Zn-Al alloys

ZHANG Jing(张 静)[1, 2], LI Zhong-sheng(李忠盛)[1], GUO Zheng-xiao[2], PAN Fu-sheng(潘复生)[1]

1. College of Materials Science and Engineering, Chongqing University, Chongqing 400044, China;
2. Department of Materials, Queen Mary, University of London, London E1 4NS, UK

Received 29 June 2005; accepted 7 December 2005

Abstract: The microstructural constituents and the crystallographic morphology of the primary intermetallic phases in permanent-mould-cast Mg-Zn-Al alloys with typical compositions within high zinc castable domain were investigated. Three kinds of primary compounds with distinct morphology were identified as $Mg_{32}(Al,Zn)_{49}$(τ), MgZn(ε), and a ternary icosahedral quasi-crystalline compound (denoted with Q). The constituent is found to change with Zn and Al content and their concentration ratio. Alloys with middle mass ratio of Zn to Al and Al content, consist of α-Mg and τ phase, while alloys with high mass ratio of Zn to Al and low Al are composed of α-Mg, ε and a small amount of τ, those with low ratio of Zn to Al and high Al consist of α-Mg with Q. Solidification characteristics and process were proposed. The solidification ranges and liquidus temperature decrease with increasing Zn and Al content for τ- and Q-type alloys, whereas ε-type alloy shows reverse tendency. The second phase transformation moves to higher temperature range when Al content increases and ratio of Zn to Al decreases.

Key words: Mg alloys; ZA alloys; Mg-Zn-Al alloys; intermetallic compounds; $Mg_{32}(Al,Zn)_{49}$; MgZn

1 Introduction

Magnesium alloy exhibits light mass, high specific strength and stiffness. Therefore, extensive application of magnesium alloys to various automobile parts is expected to enhance fuel efficiency through mass reduction. However, the unsatisfactory thermal properties restrict its application for powertrain components like automatic transmission case and engine block operating at elevated temperatures whose application could achieve more effective reductions. Popularly used commercial Mg-Al based alloys, such as AZ91, AM60 and AM50, are all prone to excess deformation at temperatures above 100℃, which is attributed to the discontinuous precipitation of $Mg_{17}Al_{12}$ phase at grain boundaries[1, 2]. To develop economic alternatives has become one of the most active research areas at the present.

Experimental zinc-rich magnesium alloys (Mg-Zn-Al) were firstly developed in 1970s, which showed better creep resistance, good castability, and great resistance to hot cracking[3]. No further investigations, however, have been carried out thereafter. Last five years has seen revived interests on Mg-Zn-Al system where new applications of magnesium castings, especially in automobile industry, which require enhanced elevated temperature creep resistance better than AZ91 in the temperature range of 100-200 ℃, while in the meantime without additional cost penalty by containing costly alloying elements to complete with relatively lower cost metals such as aluminum and steel, have emerged. Several Mg-Zn-Al based alloys, with composition typically of ZA104[4,5], ZA84[6,7], ZA52[8], have been recently developed with the evaluation of as-cast microstructure and properties. However, due to the complexity and uncertainty of Mg-rich Mg-Zn-Al ternary phase diagram[9], there is no conclusion on phase types versus compositions in high zinc magnesium alloys, discrepancies existing between different researchers as to phase types[6, 10]. Attempts to improve creep resistance through microstructure modification by identifying more promising chemical constitution are thus restricted. In order to increase the

Foundation item: Project(50301018) supported by the National Natural Science Foundation of China
Corresponding author: ZHANG Jing; Tel: +86-23-68326396; E-mail: jingzhang@cqu.edu.cn

understanding of the microstructural and solidification characteristics of this high zinc magnesium alloys, a series of ZA alloys with typical compositions within castable domain of high zinc concentration (Fig.1)[3] have been developed and permanent mould cast in the experiment. The microstructural constituent and its change with element content and ratio of Zn to Al, the crystallization morphology of the primary intermetallic phases, as well as related solidification characteristics are systematically studied, in order to obtain fundamental knowledge for new alloy design.

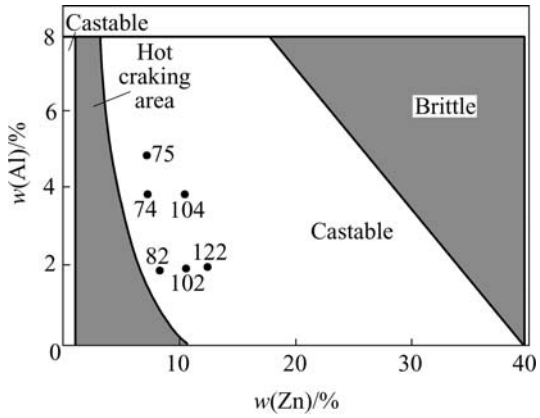

Fig.1 Castability of Mg-Zn-Al alloy system[3](Composition of experimental ZA alloys are also given in this figure by corresponding alloy notations)

2 Experimental

Within the wide castable domain of high zinc concentration, experimental alloys were selected as shown in Fig.1 based on the following rules: the content of zinc is 1%(mass fraction, the same below if not mentioned) higher than that of the boundary between hot cracking area and castable area in high zinc side. Keep the content of alloy elements as low as possible in order to maintain the advantage of mass reduction. ZA82 and ZA74 were thus determined. Four other compositions, ZA102, ZA122, ZA104, and ZA75 were also chosen with fixed Al or Zn content to compare the tendency of phase changes with the changes of the element contents of Al and Zn and the concentration ratios of Zn to Al as well.

Commercial high-purity Mg, Zn (>99.9%) and Al (>99.8%) were used to prepare the ZA series alloys. An electric resistance furnace and a steel crucible were used for melting and alloying operations. On-line protective gas generation apparatus was used to provide continuous protection during melting with a mixture of SO_2 and CO_2. The melt was homogenized by mechanical stirring. After complete mixing, the melt was kept at 700 ℃ for 5 min and then poured into a permanent mould whose temperature was maintained at 300 ℃. Chemical compositions of ingots were inspected by ICP. AZ91 alloy ingots were also cast under the same conditions for microstructrual comparison.

The microstructures of specimens etched by 8% nitric acid distilled water solution were examined by optical microscopy and SEM. X-ray diffraction characterization was conducted using a D5000 Siemens diffractometer equipped with Cu K_α radiation to identify the phase constitutions present in experimental alloys. DSC analyses were carried out using a NETZSCH STA 449C system. Samples weighed around 30 mg were heated in flowing argon atmosphere from 30 to 700 ℃, then kept for 5 min before cooling down to 100 ℃. Both heating and cooling curves were recorded at a controlled speed of 15 K/min.

3 Results and discussion

3.1 Microstructure

The typical as-cast microstructures of all the studied alloys are shown in Fig.2. In these alloys, the microstructure displays a mostly dendritic morphology with the second phases distributed in interdendritic spacings and along grain boundaries. Further detailed observation reveals that these primary intermetallic particles manifest different crystallographic characteristics, as can be seen from Fig.3. A typical microstructure of ZA82 is illustrated in Fig.2(a), only cramp lump compounds are identified in the boundary areas, which is much like a set of fish skeleton with stings and bone lumps under higher magnification (Fig.3(a)). XRD pattern of ZA82 indicates that this alloy is mainly composed of α-Mg phase and a small amount of $Mg_{32}(Al,Zn)_{49}$, also known as τ phase (Fig.4(a)), which has a body-centered cubic structure (space group $Im\bar{3}$, a=1.416 nm[10]). In ZA102 alloy, in addition to α-Mg phase and τ phase, another phase, MgZn phase, also known as ε phase, was also detected by XRD in the as-cast microstructure (Fig.4(b)). SEM observation reveals the detailed structure of the phase, as shown in Fig.3(b), which consists of many approximately paralleled white laths. Cramp lumps are also found in the boundary areas. With increasing Zn content, the boundary areas of ZA122 alloy are dominated by the wide paralleled structure eutectic phases, which likely make the boundary thicker, as obviously seen from Fig.2(c). Additionally, the dendritic structure becomes somewhat coarser with increasing zinc content. The apparent width boundary indicates that the outer part and the inner part of these boundary phases have different etching behaviors, suggesting different compositions in outer part and middle part. XRD analysis shows similar result about the microstructure of ZA122 alloy, which is mainly composed of α-Mg, ε, and a small amount of τ

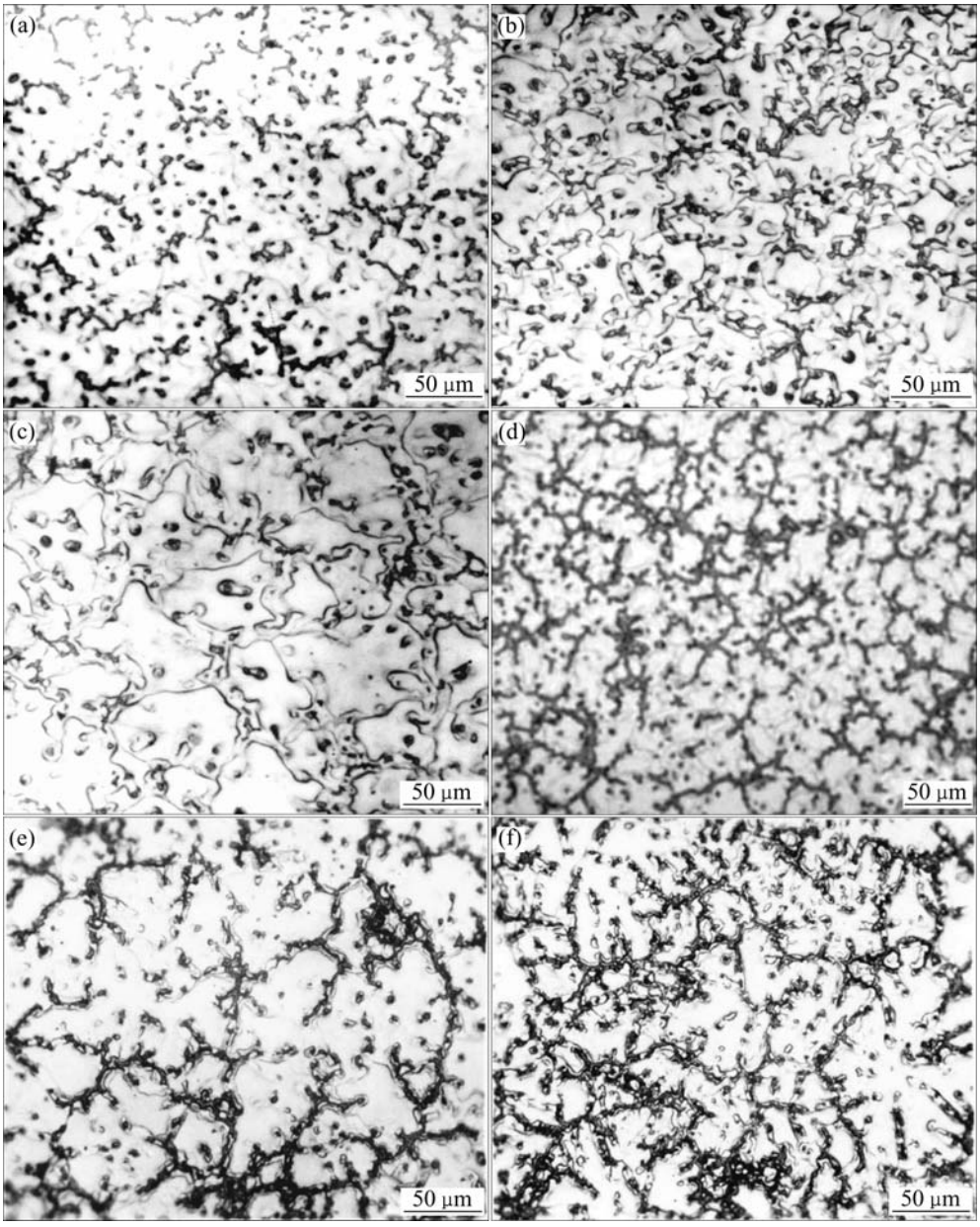

Fig.2 Optical microstructures of ZA82(a), ZA102(b), ZA122(c), ZA104(d), ZA74(e) and ZA75(f) alloys cast in permanent mould

phases (Fig.4(c)). Whereas with the increasing content of Al, the parallel structure eutectic phase present in ZA102 alloy disappears again in ZA104 alloy, whose typical as-cast structure is manifested in Fig.2(d), showing solely cramp lump compounds distributing along grain boundaries, similar to that of alloy ZA82. XRD result also shows the only intermetallic phase τ, besides the matrix α-Mg phase, present in ZA104 alloy (Fig.4(d)).

When the concentration ratio of Zn to Al moves further to lower side than that of ZA104, alloy ZA74 exhibits a completely different microstructure characteristics, as shown in Fig.2(e). Under optical microscope, the microstructure displays a kind of necklace morphology, with more or less regular black and white particles connecting into a chain. Such feature becomes even more obvious in ZA75 alloy (Fig.2(f)), when the ratio goes even lower. Further detailed observation of SEM reveals a cluster of corn-like phase marked with eyelike spots (Fig.3(c)), which might interpret the necklace feature on metallographical cross section of specimen. However, in spite of a large quantity of compounds existing in the specimens, no second phase was detected besides the α-Mg matrix phase in XRD under the same condition as the other specimens. Using electron diffraction, NIE et al[6] concluded that most primary intermetallic particles were found to be a ternary icosahedral quasi-crystalline phase in the as-cast microstructure of a similar permanent mould-cast alloy with the nominal composition of Mg-8%Zn-4%Al. Similar observations concerning the phase identification by TEM analysis were reported by VOGEL et al[11, 12] in ZA85 alloy. In this case the grain boundary quasi-

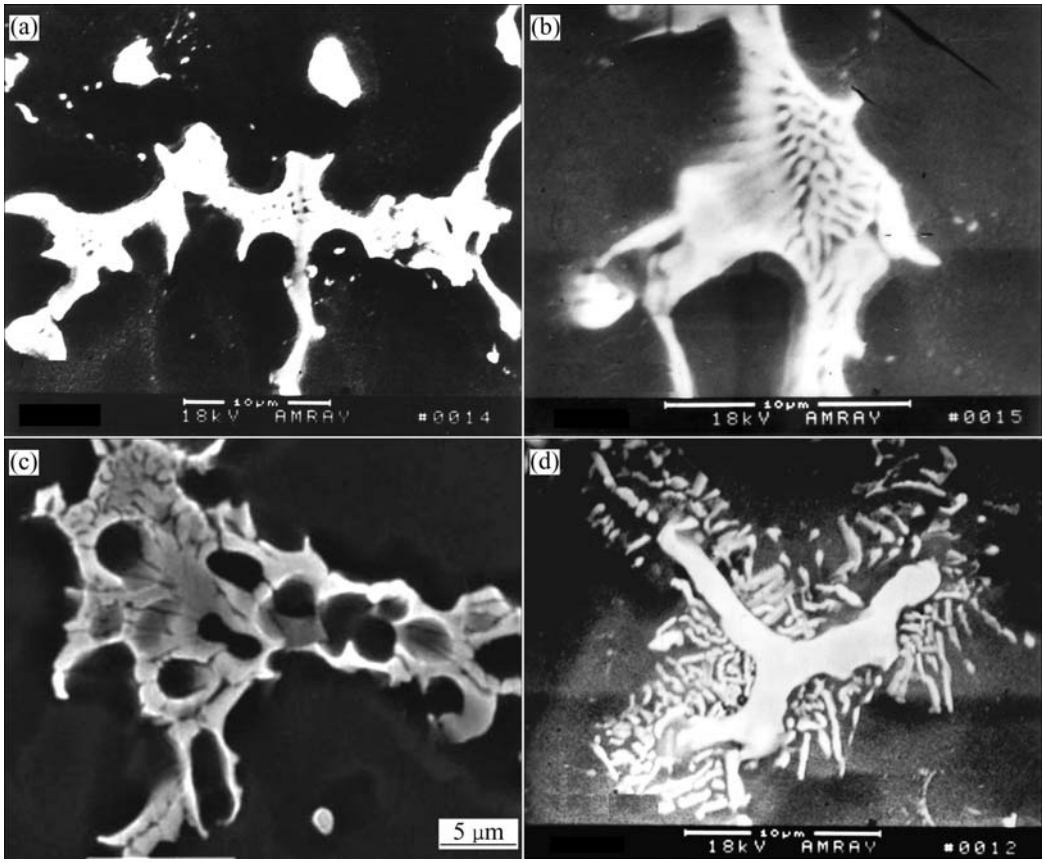

Fig.3 SEM images showing different crystallographic characteristics of secondary phases of τ(a), ε(b), and Q(c) in experimental high zinc alloys and γ(d) in AZ91 alloy

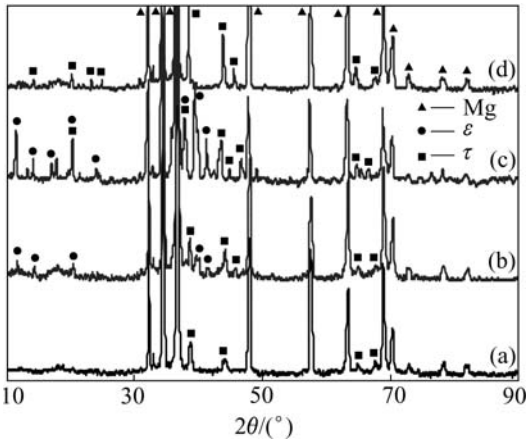

Fig.4 X-ray diffraction patterns of ZA82(a), ZA102(b), ZA122 (c) and ZA104(d)

crystalline phases were strongly supported, but its formation condition and chemical composition remain to be elucidated.

In all the experimental alloys no γ phases were found, indicating that the formation of eutectic $Mg_{17}Al_{12}$ phase is completely suppressed by high zinc. For comparison, typical morphology of γ phase is also given in Fig.3(d), recorded in AZ91 alloy, which manifests grain boundary blocky divorced eutectic particles and lamellar colonies of discontinuous precipitation during cooling. X-ray diffraction peaks of these phases were found to be somewhat shifted from the standard positions, and from each other for the same phase in different alloys as well, indicating small changes in inter-planar spacing. These differences can be ascribed to the variable concentrations of solutes in α-Mg or that of the ternary solute in binary phase MgZn, as well as the wide range of composition of ternary intermetallic phases.

As a summary, three different kinds of primary compounds form along with changing Zn and Al content and concentration ratio of Zn to Al under normal permanent mould-cast conditions, τ, ε, and quasi-crystalline phases. Accordingly, these alloys within the high zinc castable domain can then be divided into three groups as follows(shown in Fig.5): Type Ⅰ, ZA82 and ZA104, consists of α-Mg and fish bone like cramp lump τ phase; Type Ⅱ, including ZA102 and ZA122, is composed of α-Mg, τ, and binary eutectic ε phase, which is a dominant phase and characterized by its many approximately parallel laths structures; whereas Type Ⅲ, located in comparatively lower Zn/Al ratio and higher Al content part, such as ZA74 and ZA75, consists of α-Mg with icosahedral quasi-crystalline phases.

The section Ⅲ boundary in high Al side is dashdotted in Fig.5 because of the uncertainty at the present the existence range of Q in term of upper Al

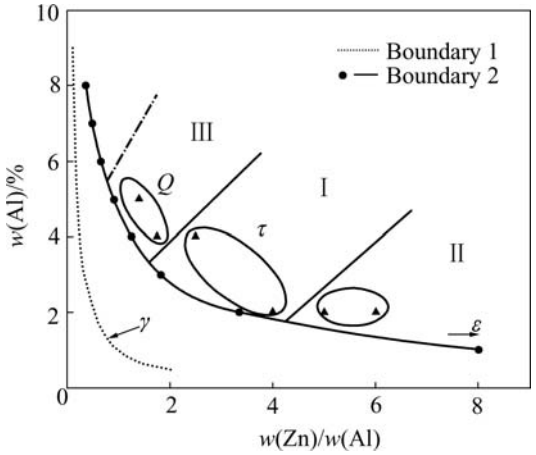

Fig.5 Schematic diagrams of microstructural constituent change with changing concentration ratio of Zn to Al and Al content: Boundaries 1 and 2 correspond to two boundaries of hot cracking area in Fig.1

limit.

3.2 Thermal analysis

To study the crystallization behaviors during solidification, DSC measurements were carried out. There are two sets of peaks in each DSC curve, corresponding to the melting of α-Mg matrix (peak Ⅰ) and the second phase transformations (peak Ⅱ), respectively. The equilibrium phase transformation temperature can be approximately calculated by averaging the two corresponding temperatures in heating curve and cooling curve, thus offsetting the temperature lags. All the characteristic temperatures emerging in the DSC curves, including the peak temperatures, the starting and ending temperatures of phase transformations, as well as the calculated equilibrium temperatures, of all the experimental alloys are listed in Table 1. Combined with the ternary phase diagram showing liquidus surface (Fig.6), the solidification process, as well as the sequence of the second phase transformations during solidification could be determined.

In ZA102, primary α(Mg) phase starts nucleation and grow the at 615 ℃ when the melt begins to solidify. the second phase reactions occur over a temperature range from 341 to 316 ℃. Three thermal events are involved. The first corresponds to a binary eutectic reaction $L_1 \rightarrow \alpha\text{-Mg}+\varepsilon+L_2$, whose peak temperature is 341 ℃. Following this is a ternary quasi-peritectic reaction $L_2+\varepsilon \rightarrow \alpha\text{-Mg}+\tau$, occurring at 334 ℃. The third peak is very weak, from which solid phase transformations, can be inferred. The final microstructure of the alloy is composed of α-Mg, ε and τ phases. The corresponding endothermal reactions in ZA102 alloy were not detected separately largely because of the variable contact resistance in heating and cooling processes.

Alloy ZA122 has similar thermal events to ZA102. In the case of ZA82, the amount of eutectic product ε should be very small and it is expected to be used up in

Table 1 Characteristic temperatures emerging in DSC curves(℃)

Alloy	Stage	Melting of matrix		Second phase transformations					Solidification range
		Peak I	Starting	Peak(s) II			Starting	Ending	
ZA82	Heating	611.9	620		341.7		352	335	
	Cooling	602.3	612		324.4		327	322	283
	Equilibrium	607.1	616		333.1		340	329	
ZA102	Heating	610.5	620		342.7		355	327	
	Cooling	600.4	610	332.4	325.5	307.8	327	307	281
	Equilibrium	605.5	615	341	334.1	316.4	341	317	
ZA122	Heating	627.1	640		342.1		350	337	
	Cooling	616.9	625		329.9		330	320	296
	Equilibrium	622.0	632		336		340	329	
ZA104	Heating	595.6	620		361.5		390	340	
	Cooling	577.6	594		338.2		350	310	257
	Equilibrium	586.6	607		349.9		370	325	
ZA74	Heating	612.3	640		369.3		398	358	
	Cooling	578.8	606		350.8		358	320	263
	Equilibrium	595.6	623		360.1		378	339	
ZA75	Heating	598.5	629		372.2		398	358	247
	Cooling	580.5	594		354.8		358	327	
	Equilibrium	589	611		363.5		378	343	

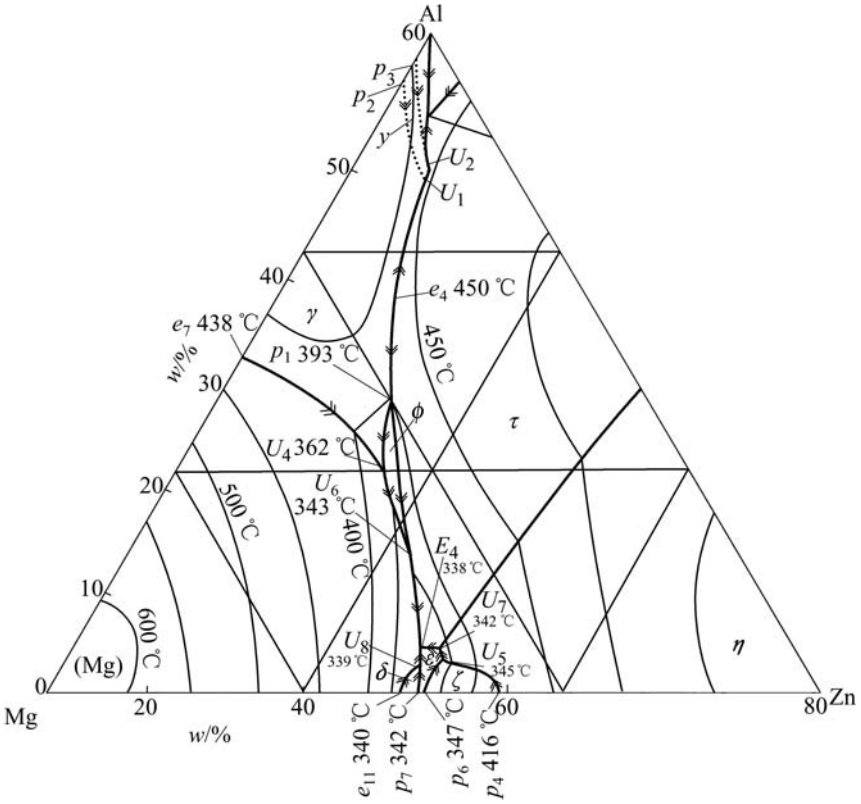

Fig.6 Liquidus projection of Mg-Zn-Al (Mg rich) ternary phase diagram[13] (Grid in mole fraction and axes in mass fraction)

the ternaryquasi-peritectic reaction. It is noteworthy that peak Ⅱ temperature increases with increasing Zn ZA102, and ZA122, respectively. It is most probably due to the different contribution fractions of each thermal event in the total thermal effect. The higher the temperature is, the greater the contribution of the first binary eutectic reaction is, which suggests that more ε product forms, also accounting for the different solidification microstructures: the least ε binary product in ZA82 results in the solely second τ phase in this alloy, whereas most ε product in ZA122 makes it a dominant compound in final microstructure. It is reasonable to infer the tendency that further increase of Zn concentration leads to solely ε second phase, which is also indicated in Fig.5. Type II alloy can thus be named ε-type high zinc magnesium alloy. Different reaction fractions in ZA82 and ZA122 with those in ZA102 may also result in inseparable and overlapping of thermal evolutions, accounting for only one detectable peak in the former two.

With increasing Al content the liquidus temperature decreases while the second phase transformation moves to higher temperature range. In alloy ZA104, solidification starts at 607 ℃. The second phase transformation starts at 370 ℃ with a binary eutectic reaction $L_1 \rightarrow \alpha\text{-Mg}+\varphi+L_2$, followed by a ternary quasi-peritectic reaction $L_2+\varphi \rightarrow \alpha\text{-Mg}+\tau+L_3$(343 ℃ in equilibrium phase diagram), and ends with another binary eutectic reaction $L_3 \rightarrow \alpha\text{-Mg}+\tau$. The amount of eutectic φ phase should be very small and is expected to be used up in the following quasi-peritectic reaction. The subsequent solidification microstructure is α-Mg+τ phases. It is worthy to mention that although alloy ZA104 and ZA82 have the same phase constituents, they undergo different solidification processes. These alloys characterized by τ compounds can also be named τ-type high zinc magnesium alloy.

To alloys with low concentration ratio of Zn to Al and high Al content, the second phase transformations occur at even higher temperature ranges. ZA74 and ZA75 have almost the same temperature range and similar thermal events during solidification evolution, both of which start at 378 ℃. According to the equilibrium phase diagram, the first is a binary eutectic reaction $L_1 \rightarrow \alpha\text{-Mg}+\gamma+L_2$, which proceeds until the residual liquid temperature reaches 362 ℃ where a ternary quasi-peritectic reaction $L_2+\gamma \rightarrow \alpha\text{-Mg}+\varphi+L_3$ occurs, and finally, the binary eutectic reaction $L_3 \rightarrow \alpha\text{-Mg}+\varphi$ takes place. The peak Ⅱ temperatures, being 360.1 ℃ and 363.5 ℃ in ZA74 and ZA75, respectively, are in good agreement with the equilibrium temperature, which strongly supports the above mentioned events,

content, being 333 ℃, 334 ℃, and 336 ℃ in alloy ZA82,

suggesting that φ is likely a stable phase in the as-cast microstructure, which is however not the case. The quasi- crystalline in thses alloys is denoted by the initial letter of *Q*. This type of alloy can also be named *Q*-type high zinc magnesium alloy. It should be mentioned that with increaseing Al content, ZA75 shows higher peak Ⅱ temperature than ZA74, indicating greater contribution of the first binary eutectic reaction to the total thermal effect, suggesting more γ phase forms. It is reasonable to infer that with further increase of Al content, γ phase can not be consumed in the following ternary quasi-peritectic reaction and will emerge in the microstructure, which is detrimental to elevated temperature creep resistance. Well-developed commercial Mg-Al-Zn alloys are characterized by γ phase, which normally contains 1%Zn, situating just at the boundary of hot cracking area of low zinc side. For comparison, this type of alloy, also named as γ-type magnesium alloy, is denoted in the diagram shown in Fig.5.

To calculate the solidification range, the starting temperature of the first peak is taken as the liquidus temperature. For solidus temperature, because the second phase transformations may involve solid reaction, the peak temperature instead of the ending temperature of which is roughly accepted. The results are shown in Table 1. All alloys have solidification ranges wider than that of AZ91 alloy, which is about 165 ℃. It can be seen from Table 1 that both the liquidus temperature and solidification range show the same tendency with changing Al and Zn content. At low Al content (2%), the liquidus temperature and solidification range decline slightly from 616 ℃ and 283 ℃ to 615 ℃ and 281 ℃ respectively with the increase of Zn content from 8 to 10%; while higher Al content (4%) leads to a more apparent decrease, 623 ℃ and 263 ℃ at 7% Zn, and 607 ℃ and 257 ℃ at 10% Zn, respectively. In contrast, both liqudus temperature and solidification range show sharp increase for ε-type alloy with increasing Zn content from 10% to 12%. With fixed Zn content of either 7% or 10%, alloys both exhibit lower liquidus temperature and narrower solidification range when Al content increases higher, that is, from 4% to 5% or from 2% to 4%, respectively.

Acknowledgement

The authors gratefully acknowledges the support of British Royal Society KC Wong Fellowship.

References

[1] HUMBLE P. Towards a cheap creep resistant magnesium alloy [J]. Materials Forum, 1997, 21: 45−56.
[2] POLMEAR I J. Light Alloys: Metallurgy of the Light Metals[M]. London: Arnold, 1995.
[3] FOERSTER G S. New developments in magnesium die casting [A]. Proceeding of the IMA 33rd Annual Meeting [C]. Montreal, Quebec, 1976. 35−39.
[4] ZHANG Z, TREMBLAY R, DUBE D. Microstructure and mechanical properties of ZA104(0.3-0.6Ca) die-casting magnesium alloys [J]. Mater Sci Eng A, 2004, A385: 286−291.
[5] ZHANG Z, TREMBLAY R, DUBE D. Microstructure and creep resistance of Mg-10Zn-4Al-0.15Ca Permanent moulding alloy [J]. Mater Sci Technol, 2002, 18: 433−437.
[6] BOURGEOIS L, MENDIS C L, MUDDLE B C, NIE J F. Characterization of quasicrystalline primary intermetallic particles in Mg-8wt% Zn-4wt% Al casting alloy[J]. Philosophical Magazine Letters. 2001, 81(10): 709−718.
[7] MENDIS C, BOURGEOIS L, MUDDLE B, NIE J F. Effects of Ca additions on microstructures, age hardening response and creep behaviour of Mg-8Zn-4Al casting alloy [A]. Magnesium Technology 2003, 2003 TMS Annual Meeting [C]. San Diego, CA, USA, 2003, 183−188.
[8] ZOU Hong-hui, ZENG Xiao-qin, ZHAI Chun-quan, DING Wen-jiang. Effects of Nd on the microstructure of ZA52 alloy[J]. Mater Sci Eng A, 2005, A392: 229−234.
[9] LIANG H, CHEN S L, CHANG Y A. A thermodynamic description of the Al-Mg-Zn system[J]. Metall Mater Trans A, 1997, A28: 1725−1734.
[10] BOURGEOIS L, MUDDLE B C, NIE J F. The crystal structure of the equilibrium φ phase in Mg-Zn-Al casting alloys[J]. Acta Mater, 2001, 49: 2701−2711.
[11] VOGEL M, KRAFT O, DEHM G, ARZT E. Quasi-crystalline grain-boundary phase in the magnesium die-cast alloy ZA85[J]. Scripta Materialia, 2001, 45: 517−524.
[12] VOGEL M, KRAFT O, ARZT E. Creep behavior of magnesium die-cast alloy ZA85[J]. Scripta Materialia, 2003, 48: 985−990.
[13] PETROV D V. Aluminum-Magnesium-Zinc. Ternary Alloys: A Comprehensive Compendium of Evaluated Constitutional Data and Phase Diagrams (Vol.7)[M]. Weinheim: VCM, 1993. 57−71.

(Edited by LONG Huai-zhong)